Electrochemistry Communications 12 (2010) 1674–1677

Contents lists available at ScienceDirect

Electrochemistry Communications

journal homepage: www.elsevier.com/locate/elecom

Nano-structured $Li_3V_2(PO_4)_3$/carbon composite for high-rate lithium-ion batteries

Anqiang Pan [a,b], Jun Liu [b,*], Ji-Guang Zhang [b,*], Wu Xu [b], Guozhong Cao [c], Zimin Nie [b], Bruce W. Arey [b], Shuquan Liang [a,*]

[a] Department of Materials Science and Engineering, Central South University, Changsha, Hunan 410083, China
[b] Pacific Northwest National Laboratory, Richland, WA 99352, USA
[c] Department of Materials Science and Engineering, University of Washington, Seattle, WA 98195, USA

ARTICLE INFO

Article history:
Received 14 July 2010
Received in revised form 13 September 2010
Accepted 14 September 2010
Available online 22 September 2010

Keywords:
Li-ion batteries
Cathode
Vanadium phosphate
$Li_3V_2(PO_4)_3$
High-power battery

ABSTRACT

Nano-structured $Li_3V_2(PO_4)_3$/carbon composite ($Li_3V_2(PO_4)_3$/C) has been successfully prepared by incorporating the precursor solution into a highly mesoporous carbon with an expanded pore structure. X-ray diffraction analysis, scanning electron microscopy, and transmission electron microscopy were used to characterize the structure of the composites. $Li_3V_2(PO_4)_3$ had particle sizes of <50 nm and was well dispersed in the carbon matrix. When cycled within a voltage range of 3 to 4.3 V, a $Li_3V_2(PO_4)_3$/C composite delivered a reversible capacity of 122 mA h g^{-1} at a 1C rate and maintained a specific discharge capacity of 83 mA h g^{-1} at a 32C rate. These results demonstrate that cathodes made from a nano-structured $Li_3V_2(PO_4)_3$ and mesoporous carbon composite material have great potential for use in high-power Li-ion batteries.

1. Introduction

Rechargeable Li-ion batteries are the power sources for modern electronic applications because of their high energy density and long cycle life. Recently, the lithium transition metal phosphates (such as $LiFePO_4$, $LiMnPO_4$, and $Li_3V_2(PO_4)_3$) have attracted great interest among researchers because of their appealing features, like good electrochemical and thermal stabilities and high operation potentials [1–4]. $Li_3V_2(PO_4)_3$ consists of a three-dimensional framework of slightly distorted VO_6 octahedra and PO_4 tetrahedra that share oxygen vertexes hosting lithium ions in relatively large interstitial sites [5,6]. It also exhibits exceptional ionic conductivity that results from the large interstitial spaces created by PO_4^{3-} units, which allows fast ion migration in three dimensions. Three reversible lithium ions can be totally extracted from the lattice of $Li_3V_2(PO_4)_3$ within a range of 3.0 and 4.8 V, and the highest theoretical capacity of 197 mA h g^{-1} among the lithium metal phosphates can be obtained from this material. Compared to $LiFePO_4$, which has an olivine-type structure and a curved one-dimensional channel for lithium-ion diffusion, monoclinic $Li_3V_2(PO_4)_3$ provides better electrochemical performance because it exhibits a three-dimensional path for lithium-ion diffusion [7]. Rui et al. [5] reported that the Li^+ diffusion coefficiency (D_{Li+}) in $Li_3V_2(PO_4)_3$ ranged from 10^{-9} to 10^{-10} cm^2 s^{-1}, which is five times more than the D_{Li+} of $LiFePO_4$ (i.e., 10^{-14} to 10^{-16} cm^2 s^{-1}) reported by Prosini et al. [8]. This indicates that $Li_3V_2(PO_4)_3$ has a great potential to achieve a higher rate capability than $LiFePO_4$. However, the intrinsic low electronic conductivity (i.e., 2.4×10^{-7} S cm^{-1}at room temperature) of $Li_3V_2(PO_4)_3$ significantly limits its rate performance [5]. Various synthesis and processing approaches, such as alien metal doping and carbon coating [5,9–11], have been employed to solve this problem. All materials produced using these methods exhibit better capacity retention and higher specific capacity than that of pure $Li_3V_2(PO_4)_3$ powders. However, the rate performance of $Li_3V_2(PO_4)_3$ is still not satisfactory because its particles are not really nano-sized. Further reducing the particle size to reduce Li-ion diffusion and electron-transportation distance would improve the rate performance of the electrode because, in accordance with Fick's law, the diffusion time is proportional to the square of the diffusion distance. Wang et al. [12,13] reported that nano-structured SnO_2/carbon and Si/carbon composites showed superior lithium intercalation properties because of the size of refined active particles and the good conductive media of carbon. Also, Doherty et al. report that $LiFePO_4$ electrode materials with hierarchically porous structure had high-power capability for lithium-ion batteries, but the synthesis of which is complicated and needs careful handling [14]. Thus, finding a facile and large scale available production method by effectively embedding nano-sized $Li_3V_2(PO_4)_3$ particles in the mesoporous carbon matrix would be an attractive approach to improve the power performance of $Li_3V_2(PO_4)_3$ cathode materials. In this regard, Ketjenblack carbon (EC600JD, Akzo Nobel, (referred to as KB hereafter) is an excellent candidate due to its high surface area, mesoporous structure, easy dispersion, good conductivity and cost effective. It has been used as the electrode material for fuel cells and Li-air batteries as well as the conductive additive in Li-ion batteries [15–17].

* Corresponding authors.
E-mail addresses: jun.liu@pnl.gov (J. Liu), jiguang.zhang@pnl.gov (J.-G. Zhang), lsq@mail.csu.edu.cn (S. Liang).

1388-2481/$ – see front matter © 2010 Published by Elsevier B.V.
doi:10.1016/j.elecom.2010.09.014

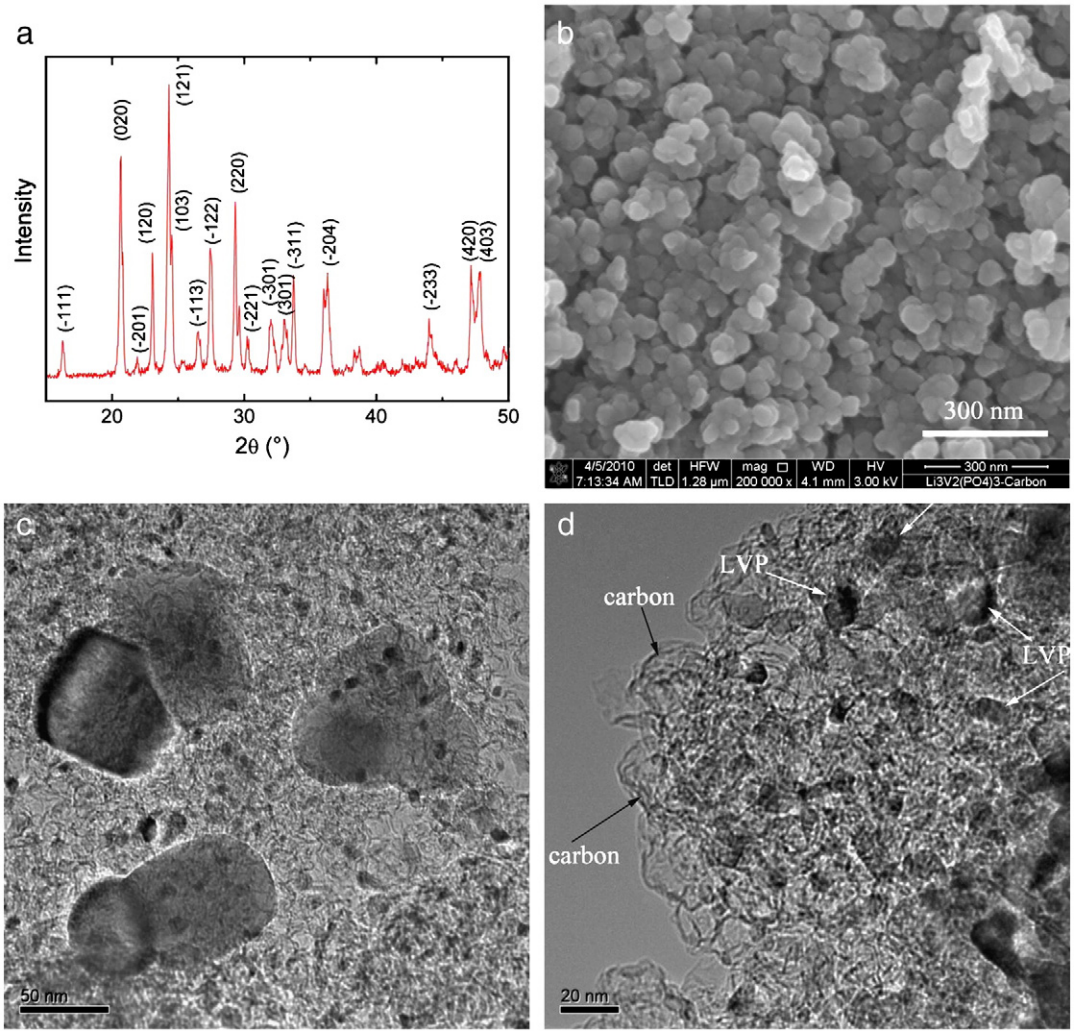

Fig. 1. XRD (a), SEM (b), and TEM (c, d) images of the as-prepared $Li_3V_2(PO_4)_3$/C composite sample.

In this paper, we report a novel approach for fabricating a nano-scale $Li_3V_2(PO_4)_3$/C composite. This approach involves adsorbing a $Li_3V_2(PO_4)_3$ precursor solution into the expanded mesopores of KB carbon, which inhibits particle aggregation during the preparation process and serves as good conductive carbon in the electrode. The electrochemical performances, especially at the high-power discharge rates of the successfully synthesized nano-sized $Li_3V_2(PO_4)_3$/C composite material, have been studied.

2. Experimental

All chemicals used in this work were of analytical grade. V_2O_5, $NH_4H_2PO_4$, Li_2CO_3, and oxalic acid were used as-received to prepare the precursor solution. Oxalic acid was used both as a chelating agent and a reducing agent. First, V_2O_5 and oxalic acid in a stoichiometric ratio of 1:3 were dissolved in deionized water under magnetic stirring at room temperature until a clear blue solution was formed. Second, a mixture of stoichiometric $NH_4H_2PO_4$ and Li_2CO_3 was added to the solution, and this batch was vigorously stirred using a magnetic stirrer for 1 h. KB carbon was then added to the solution, and the mixture was heated to 70 °C under active stirring to evaporate the water for several hours until a homogenous slurry was formed. Finally, the slurry was transferred to and kept in an oven at 80 °C overnight to obtain dry solids. The amount of KB carbon added into the precursor during the preparation was based on the carbon content in the final $Li_3V_2(PO_4)$/carbon composite. In this work, 20% carbon in the final $Li_3V_2(PO_4)$/carbon composite was added, and there was no carbon loss during the whole process as indicated by the thermal gravimetric analysis results. The resulting material was pressed into pellets and calcined at 350 °C for 4 h under a gas flow composed of 96% Ar and 4% H_2. Finally, the calcined material was reground, repressed into pellets, and sintered at 800 °C for 8 h in a tube furnace under a gas flow composed of 96% Ar and 4% H_2 to give the $Li_3V_2(PO_4)_3$/C composite.

The crystalline structure of the as-prepared sample was determined by X-ray diffraction (XRD) analysis using a Scintag XDS2000 θ–θ powder diffractometer equipped with a Ge (Li) solid-state detector and a Cu Kα sealed tube (λ = 1.54178 Å). The sample was scanned in the range between 10 and 70° (2θ), with a step size of 0.02° and an exposure time of 10 s. Scanning electron microscopy (SEM) (FEI Helios 600 Nanolab FIB-SEM, 3 KV) was used to characterize the particle morphology. High-resolution transmission electron microscopy (TEM) analysis was carried out on a Jeol JEM 2010 microscope fitted with a LaB_6 filament and an acceleration voltage of 200 kV.

The $Li_3V_2(PO_4)_3$/C composite was mixed with a poly(vinylidene fluoride) binder in a weight ratio of 90:10 without adding extra carbon and then dispersed in *N*-methylpyrrolidone solution to make a slurry composed of active material/carbon/binder in a ratio of 72:18:10. The slurry was coated on an Al foil and dried in a vacuum oven at 100 °C overnight before coin cell assembly. The tap density of the $Li_3V_2(PO_4)_3$/carbon composite was about 0.6 g/mL, and its loading on the Al current collector was 1–2 mg cm^{-2}. The half-cells (2325 coin cell, National Research Council, Canada) were assembled in a glove box (MBraun, Inc.)

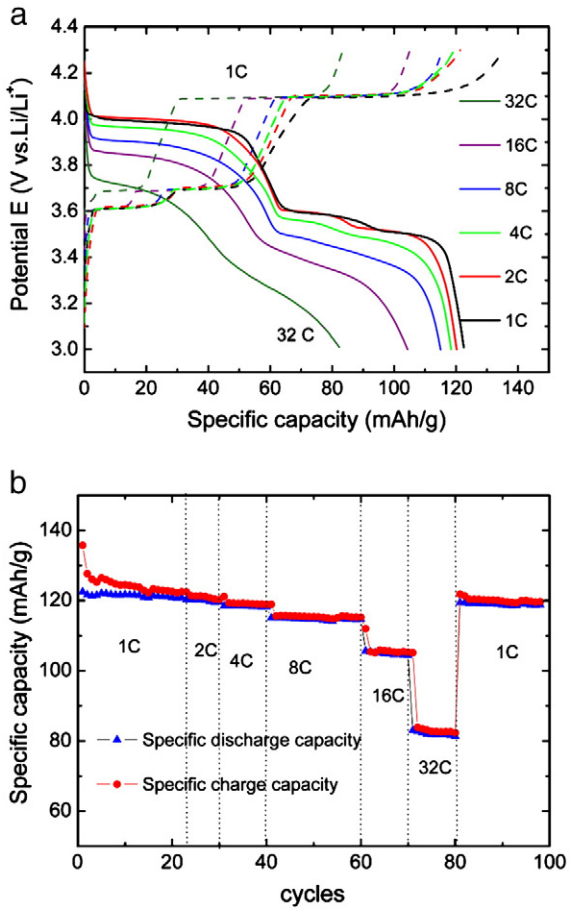

Fig. 2. (a) Discharge/charge curves and (b) cycling performance at various discharge rates with constant charge at 1C (140 mA g^{-1}) of the $Li_3V_2(PO_4)_3$/C composite material.

filled with ultra-high-purity argon using a polypropylene membrane (Celgard 3501) as the separator, lithium metal as the anode, and 1-M $LiPF_6$ in ethyl carbonate/dimethyl carbonate (1:1 v/v ratio) as the electrolyte. The electrochemical performance of the $Li_3V_2(PO_4)_3$/C composite was evaluated on an Arbin Battery Tester BT-2000 (Arbin Instruments, College Station, TX) at room temperature. The half-cells were tested in a voltage cutoff of 3 to 4.3 V vs. Li/Li^+ at various C-rates based on the weight of $Li_3V_2(PO_4)_3$ (assuming 1C = 140 mAh g^{-1}).

3. Results and discussion

XRD, SEM, and TEM images of the as-prepared $Li_3V_2(PO_4)_3$/C composite sample are shown in Fig. 1. The main peaks of the XRD pattern are indexed in Fig. 1a, and all peaks detected correspond well to the peaks reported previously in the literature [5]. The diffraction peaks can be assigned to monoclinic $Li_3V_2(PO_4)_3$ with the space group P21/n. No secondary phase was detected, which indicates that carbon in the composite is in an amorphous state.

As shown in the SEM image (Fig. 1b), nano-scale particles are clearly present. In the TEM images (Fig. 1c and d), two different particle sizes are observed. The larger particles are around 50 nm, which is ascribed to the particles grown on the outside of the mesopore structure of the KB carbon. These particles grew with less restriction in the mesopore structure. However, they are much smaller than the ~400-nm particles reported in the literature [11], which were produced using a similar method that did not include the addition of liquid precursor sources into the mesopore carbon during the preparation process. Much smaller particles well dispersed in the carbon matrix are predominant in the TEM images. Fig. 1d gives a clearer picture of the small $Li_3V_2(PO_4)_3$ particles embedded into the highly porous KB carbon. Most of the smaller particles as indicated by the white arrows are about 20 nm, and these smaller particles are surrounded by the carbon matrix indicated by the black arrows. This novel structure indicates the successful fabrication of a nano-structured $Li_3V_2(PO_4)_3$/C composite by absorbing the precursor solution into the mesoporous structure of the KB carbon and effectively limiting particle aggregation by the mesopores of the carbon.

Fig. 2a shows the discharge/charge curves of the $Li_2V_3(PO_4)_3$/C composite at different discharge rates and a constant charging rate of 1C. For the charge curves at a 1C rate (140 mA g^{-1}), three plateaus at 3.62, 3.70, and 4.12 V are observed, which correspond to the extraction of lithium ions and the phase transition of $Li_xV_2(PO_4)_3$ from X = 3.0 to 2.5, 2.0, and 1.0, respectively. The first lithium ion is extracted in two steps (3.62 and 3.70 V) because of the existence of an ordered phase $Li_{2.5}V_2(PO_4)_3$ at a mixed V^{3+}/V^{4+} state. Then, a single step removal of the second lithium ion at 4.12 V can be observed, which corresponds to the complete oxidation of V^{3+} to V^{4+}. Three corresponding plateaus at 4.0, 3.63, and 3.55 V during the discharge process are attributed to reinsertion of two lithium ions that accompanied the phase transition of $Li_xV_2(PO_4)_3$ from X = 1.0 to 1.5, 2.0, and 3.0. An initial discharge capacity of 122 mAh g^{-1} was obtained between 3 and 4.3 V, and the coulombic efficiency reached 90%. The capacity is higher than the 110 mA h g^{-1} of the bulk $Li_3V_2(PO_4)_3$ at C/5 as reported by Ren et al. [11]. After cycling 22 cycles at a 1C charging rate (shown in Fig. 2b), the cell retained a specific discharge capacity of 120 mA h g^{-1}. No difference in the discharge capacity was observed between 1C and 2C discharging rates. When operated at 4C and 8C discharging rates, the specific discharge capacities were 118 mA h g^{-1} and 115 mA h g^{-1}, respectively. The capacity difference between the 1C and 8C charging rates was only 5 mA h g^{-1} as shown in Fig. 2b. Even at higher discharging rates (16C and 32C), the cell still delivered specific discharge capacities of 105 mA h g^{-1} and 83 mA h g^{-1}, respectively. After 80 cycles (shown in Fig. 2b), the electrode still had a specific discharge capacity of 119 mA h g^{-1} when reset to a 1C discharging rate, which is almost the same as the discharge capacity after 22 cycles before the high-rate discharge. The excellent rate performance and good capacity retention (shown in Fig. 2b) at various discharge rates are attributed to the novel structure of the $Li_2V_3(PO_4)_3$/C composite because the nano-sized particles (20 to 50 nm) reduce the diffusion distance for the lithium ions, and the particles are well dispersed in the carbon matrix, which verifies good conductivity of the active material (as shown in Fig. 1d).

Recently, a $Li_3V_2(PO_4)_3$/C thin-film composite was produced using electrostatic spray deposition, and a particle size of ~50 nm was reported [18]. This material exhibited a good high-rate performance with a specific capacity of 80 mA h g^{-1} at a 24C rate (118 mA g^{-1} at a 1C rate), which is among the best rate performances for $Li_3V_2(PO_4)_3$/C composite materials. However, this thin-film preparation process is difficult to scale up for high-capacity applications. In our case, the bulk composite electrode exhibits even better rate performance with specific capacities of 105 mA h g^{-1} and 83 mA h g^{-1} at 16C and 32C rates, respectively. The main reasons for this superior rate performance and good cycle stability are the nano-structured particles (20 to 50 nm) and the good contact of the particles with the KB carbon matrix. Our experiments demonstrate a facile and cost-effective way to synthesize a $Li_3V_2(PO_4)_3$/C composite cathode material that has a potential use in high-power lithium-ion battery applications (e.g., for use in electric vehicles and hybrid electric vehicles).

4. Conclusions

A nano-structured $Li_3V_2(PO_4)_3$/C composite material with particle sizes < 50 nm has been successfully synthesized. The $Li_3V_2(PO_4)_3$ particles are well dispersed in the KB carbon matrix. The as-synthesized cathode material exhibits excellent rate performance and capacity retention, which can be attributed to the reduced dimensions of $Li_3V_2(PO_4)_3$ particles and the existence of a good conductive carbon matrix in the composite. These novel nano-structured $Li_3V_2(PO_4)_3$/carbon composites

have a great potential use as cathode materials for high-power lithium-ion batteries.

Acknowledgments

We acknowledge financial supports from the National Nature Science Foundation of China (No. 50774097), the Laboratory Directed Research and Development Program at Pacific Northwest National Laboratory (PNNL), and the Office of Vehicle Technologies of the U.S. Department of Energy (DOE). A.Q. Pan appreciates the financial support provided by the Chinese Scholarship Council. The SEM and TEM were performed at the Environmental Molecular Sciences Laboratory, a national scientific-user facility sponsored by the DOE's Office of Biological and Environmental Research and located at PNNL. PNNL is operated for the U.S. Department of Energy by Battelle under Contract DE-AC05-76RL01830.

References

[1] S.C. Yin, H. Grondey, P. Strobel, H. Huang, L.F. Nazar, J. Am. Chem. Soc. 125 (2003) 326.
[2] A. Yamada, S.C. Chung, K. Hinokuma, J. Electrochem. Soc. 148 (2001) A224.
[3] D.Y. Wang, H. Buqa, M. Crouzet, G. Deghenghi, T. Drezen, I. Exnar, N.H. Kwon, J.H. Miners, L. Poletto, M. Graetzel, J. Power Sources 189 (2009) 624.
[4] J. Xiao, W. Xu, D. Choi, J.-G. Zhang, J. Electrochem. Soc. 157 (2010) A142.
[5] X.H. Rui, N. Ding, J. Liu, C. Li, C.H. Chen, Electrochim. Acta 55 (2010) 2384.
[6] S.C. Yin, H. Grondey, P. Strobel, M. Anne, L.F. Nazar, J. Am. Chem. Soc. 125 (2003) 10402.
[7] S. Patoux, C. Wurm, M. Morcrette, G. Rousse, C. Masquelier, J. Power Sources 119 (2003) 278.
[8] P.P. Prosini, M. Lisi, D. Zane, M. Pasquali, Solid State Ionics 148 (2002) 45.
[9] A.P. Tang, X.Y. Wang, S.Y. Yang, J.Q. Cao, J. Appl. Electrochem. 38 (2008) 1453.
[10] L.J. Wang, X.C. Zhou, Y.L. Guo, J. Power Sources 195 (2010) 2844.
[11] M.M. Ren, Z. Zhou, X.P. Gao, W.X. Peng, J.P. Wei, J. Phys. Chem. C 112 (2008) 5689.
[12] Z. Wang, M.A. Fierke, A. Stein, J. Electrochem. Soc. 155 (2008) A658.
[13] Z. Wang, F. Li, N.S. Frgang, A. Stein, Carbon 46 (2008) 1702.
[14] C.M. Doherty, R.A. Caruso, B.M. Smarsly, C.J. Drummond, Chem. Mater. 21 (2009) 2895.
[15] M. Neergat, A.K. Shukla, J. Power Sources 104 (2002) 289.
[16] J. Xiao, D. Wang, W. Xu, D. Wang, R.E. Williford, J. Liu, J.-G. Zhang, J. Electrochem. Soc. 157 (2010) A487.
[17] D. Choi, D.H. Wang, V.V. Viswanathan, I.T. Bae, W. Wang, Z.M. Nie, J.-G. Zhang, G.L. Graff, J. Liu, Z.G. Yang, T. Duong, Electrochem. Commun. 12 (2010) 378.
[18] L. Wang, L.C. Zhang, I. Lieberwirth, H.W. Xu, C.H. Chen, Electrochem. Commun. 12 (2010) 52.